PARAMAGNETIC RESONANCE SPECTRUM OF Mn^{++} — Na^{+} VACANCY PAIR IN NaCl: Mn^{++} SINGLE CRYSTALS

By A. Jankowska

Institute of Physics, Polish Academy of Sciences, Warsaw*

(Received November 13, 1969)

The spectrum of the Mn^{++}—Na^{+} vacancy complex, in which a vacancy is at one of the twelve nearest neighbour positions with respect to the Mn^{++} ion, in quenched NaCl single crystals at liquid nitrogen temperature is described. The spin Hamiltonian constants at 77°K have been obtained as follows: $A = -87.9$ G, $a = -2.4$ G, $D = 124.3$ G, and $E = 46.2$ G. The observed angular dependence of the fine structure lines has been compared with the calculated one. The instability of the complex dependent on impurity concentration has been analyzed.

Introduction

Investigations of the paramagnetic resonance spectra of magnetic impurities in diamagnetic crystals give some information about their electronic states in crystals. Since the electronic states strongly depend on the crystal field, the state of the environment around the magnetic ions may be found by analyzing the structure of their resonance lines. In the experiment described in this paper divalent manganese was added into the monovalent lattice of sodium chloride single crystals. Manganese substitutes sodium ions in the lattice. Such an impurity disturbs the balance of charge. The requirement of charge neutrality in the whole volume of the crystal stimulates that an equal number of negatively charged defects must be simultaneously introduced. Different kinds of defects may be considered. In the absence of other negatively charged chemical impurities the most probable defect which satisfies the principle of charge compensation is the positive-ion vacancy (this is, however, but one of the possible charge compensations which may occur). Controlled numbers of positive-ion vacancies can be introduced by adding a definite quantity of divalent impurity.

Paramagnetic resonance studies can provide knowledge on the properties of the positive-ion vacancy. From this point of view the problem has been given considerable attention in many papers [1–4]. Schneider and Caffyn were the first who investigated the EPR spectrum

* Address: Instytut Fizyki PAN, Warszawa, Zielna 37, Polska.

of Mn^{++} in single crystals of NaCl [5] and [6]. Detailed considerations have been made by Morigaki *et al.* [7] and by Watkins [8–10].

This paper will deal with only the simple associated pair: Mn^{++}-vacancy in the nearest cation site, for such defects are encountered most often (Fig. 1).

Theory of the spectrum

For divalent manganese the shell of $3d$-electrons responsible for paramagnetism is just half-filled by the five electrons of this ion, and the resultant orbital angular momentum L is zero. Thus the ground state of Mn^{++} is ${}^6S_{5/2}$, and one would expect it to be slightly affected by ion environment. In ionic crystals, such as sodium chloride crystals, the spectroscopic splitting factor g should be isotropic and very close to the free electron value, crystalline field splittings should be relatively small, and the hyperfine constant nearly isotropic.

The NaCl crystal consists of two face-centered cubic lattices (one for Na^+ and the other for Cl^-) shifted by half lattice distance. When Mn^{++} is introduced into the NaCl lattice it

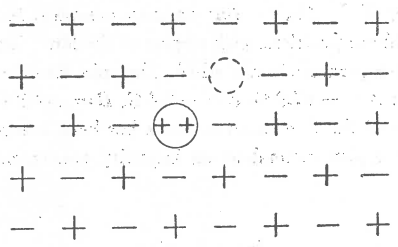

Fig. 1. Divalent manganese substitutes monovalent sodium ion. Charge compensation arises from positive ion vacancy in the nearest cation site

occupies the Na^+ site and will induce a Na^+ ion vacancy. The first nearest Na^+ ion vacancy to Mn^{++} creates the more probable vacancy complex. The environment of Mn^{++} will no longer have cubic structure. Now, there are twelve equally probable positions for vacancy around each Mn^{++} ion, what give six equally probable sets of principal axes of the Mn^{++}-vacancy complex (Fig. 2). Each set consists of two of the six [110] directions (z and x-axes) and one of the cubic axes (1), (2) or (3) (y-axis), which go together to make a rectangular system.

Then with the Zeeman energy, crystal field operator and the hyperfine interaction with one hundred percent Mn^{55} abundance (nuclear spin 5/2) the total spin Hamiltonian for the Mn^{++} ion can be written:

$$\mathcal{H} = g\beta \boldsymbol{H} \cdot \boldsymbol{S} + \mathcal{H}_{\text{cryst}} + A\boldsymbol{I} \cdot \boldsymbol{S} \qquad (1)$$

where g is the spectroscopic splitting factor, β is the Bohr magneton, H the external magnetic field, and A the hyperfine coupling constant.

The crystal field H_{cryst} includes a cubic field term, H_{cubic}, axial field term, H_{axial}, and orthorhombic field term, H_{orth}. The first field is connected with the cubic structure of the

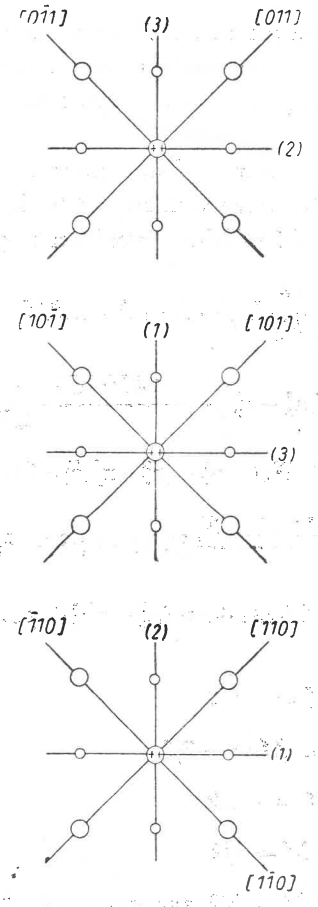

Fig. 2. Six sets of principal axes connected with twelve equally probable positions for the vacancy. (*1*), (*2*), (*3*) are the cubic coordinate axes at right angles of the crystal. The *z*-axis is taken as the direction of the Mn^{++}-vacancy complex. The large circles are cations, the small circles anions

	x	*y*	*z*
(*a*)	[0$\bar{1}$1]	[100]	[011]
	[011]	[100]	[01$\bar{1}$]
(*b*)	[10$\bar{1}$]	[010]	[101]
	[101]	[010]	[$\bar{1}$01]
(*c*)	[$\bar{1}$10]	[001]	[110]
	[110]	[001]	[1$\bar{1}$0]

NaCl crystal, whereas the other two with vacancy defects destroying the cubic symmetry near the Mn^{++} ion.

$$\mathcal{H}_{\text{cryst}} = \mathcal{H}_{\text{cubic}} + \mathcal{H}_{\text{axial}} + \mathcal{H}_{\text{orth}} \tag{2}$$

$$\mathcal{H}_{\text{cryst}} = \frac{1}{6}a\left[S_1^4+S_2^4+S_3^4-\frac{1}{5}S(S+1)\,(3S^2+3S-1)\right] + \\ +D\left[S_z^2-\frac{1}{3}S(S+1)\right] + E(S_x^2-S_y^2), \tag{3}$$

where a is the cubic field splitting parameter, D is the axial field splitting constant and the parameter E is associated with departures from the axial symmetry to the orthorhombic symmetry. S_1, S_2, S_3 and S_x, S_y, S_z are the spin components in the cubic and x, y, z coordinates, respectively.

If n_x, n_y, n_z are the direction cosines of the external magnetic field with respect to the x, y, z axes, and n_1, n_2, n_3 are the same with respect to the cubic (1), (2), (3) axes, the resonance field for the electronic $M \leftrightarrow M+1$ transition is given by

$$H = H_0 - Am - \frac{A^2}{2H_0}[I(I+1) - m^2 + m(2M+1)] - \frac{2M+1}{2} \times$$

$$\times [D(3n_z^2 - 1) + 3E(n_x^2 - n_y^2)] - \frac{24M(M+1) - 4S(S+1) + 9}{2H_0} \times$$

$$\times [D^2 n_z^2(1 - n_z^2) + E^2\{1 - n_z^2 - (n_x^2 - n_y^2)^2\} - 2DEn_z^2(n_x^2 - n_y^2)] -$$

$$- \frac{[2S(S+1) - 6M(M+1) - 3]}{8H_0}[D^2(1 - n_z^2)^2 + E^2\{4n_z^2 + (n_x^2 - n_y^2)^2\} +$$

$$+ 2DE(1 + n_z^2)(n_x^2 - n_y^2)] + cpa. \qquad (4)$$

Here

$$c = 2 \text{ for } M = -5/2$$

$$c = -5/2 \text{ for } M = -3/2$$

$$c = 0 \text{ for } M = -1/2$$

$$c = 5/2 \text{ for } M = 1/2$$

$$c = -2 \text{ for } M = 3/2 \text{ and } p = 1 - 5(n_1^2 n_2^2 + n_1^2 n_3^2 + n_2^2 n_3^2).$$

M and m are the electronic and nuclear azimuthal quantum numbers, respectively, $H_0 = h\nu_0/g\beta$ (ν_0 is the klystron frequency) and values of A, D, E, a are divided by a factor of $g\beta$ from those in Eqs (1) and (3).

The five electronic transitions (selection rule $\Delta M = \pm 1$), become split into six hyperfine lines each (selection rule $\Delta m = 0$) by hyperfine interaction, and the six sets of principal axes give, in general, a spectrum consisting of 180 lines for an arbitrary orientation of the crystal with respect to the applied magnetic field. In our experiments there are four sets of principal axes and the maximum number of lines is 120 (see next section).

Experimental methods

All the NaCl : Mn^{++} single crystals examined in this work were kindly supplied by Mr I. Olichwierowicz from the Institute of Physics of the Warsaw Technical University.

The crystals were grown by pulling from the melt at a temperature of about 800°C in air atmosphere. Doping was accomplished by mixing manganous chloride (about 10^{-3} mole fraction) and sodium chloride powders before melting. The pulling lasted about five hours

and then the specimen was cooled during another five hours. Boules obtained thus are about 3–4 centimeters long and about 1–2 centimeters in diameter.

Measurements were made by means of an X-band EPR spectrometer (9.2 GHz) with TE_{102} transmission cavity and phase-sensitive detection. 100 kHz magnetic field modula-

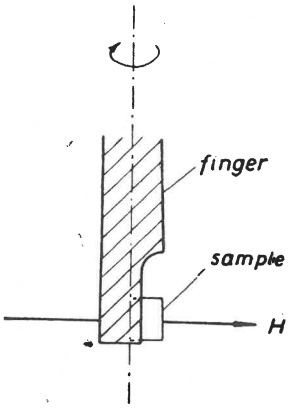

Fig. 3. The position of the sample in the magnetic field. $H = [\cos\alpha, \sin\alpha, 0]$, where α is the measured angle in the horizontal plane between the H and (1) axes

tion, small with respect to the line width of the resonance spectrum, was used. The recorded signals were proportional to the first derivatives of the absorption lines. The sweep of the external magnetic field was about 2000 G. A sample of $MgO:Mn^{++}$ powder was used as a field marker.

The preparation of the sample was as follows. The specimen of $NaCl:Mn^{++}$ was cracked into samples of dimentions about $3\times2\times1$ mm^3. Next, samples which had the best cleavage planes were selected, that is, those which were supposedly single crystals. The single crys-

TABLE I

n_x	n_y	n_z
$-\sin\alpha/\sqrt{2}$	$\cos\alpha$	$\sin\alpha/\sqrt{2}$
$\sin\alpha/\sqrt{2}$	$\cos\alpha$	$\sin\alpha/\sqrt{2}$
$\cos\alpha/\sqrt{2}$	$\sin\alpha$	$\cos\alpha/\sqrt{2}$
$\cos\alpha/\sqrt{2}$	$\sin\alpha$	$-\cos\alpha/\sqrt{2}$
$(-\cos\alpha+\sin\alpha)/\sqrt{2}$	0	$(\cos\alpha+\sin\alpha)/\sqrt{2}$
$(\cos\alpha+\sin\alpha)/\sqrt{2}$	0	$(\cos\alpha-\sin\alpha)/\sqrt{2}$

tals, annealed at a high temperature (about 600°C) for about three hours, were taken out from the heater and quenched to room temperature. Then the sample was mounted to the end of a polystyrene finger dipped into a Dewar vessel with liquid nitrogen. The sample could be oriented with respect to the magnetic field by rotating the polystyrene finger perpendicularly to the field (Fig. 3).

The direction cosines of the magnetic field with respect to the direction of the vacancy-Mn^{++} complex is given by the formula:

$$n_w = \cos(\vec{H}, \vec{w}) = \frac{\vec{H}\vec{w}}{|\vec{H}|\,|\vec{w}|},$$

where $\vec{w}$ stands for the respective unit vector of the x, y, z axes.

In Table I are the values of the direction cosines for $\vec{H} = [\cos\alpha, \sin\alpha, 0]$ and the six sets of principal axes from Fig. 2.

Equation (4) contains only the squares of n_x, n_y and n_z, so the first two sets of direction cosines are equivalent. The same is true for the next two sets. Therefore in our experiments there are only four different parts of the spectrum.

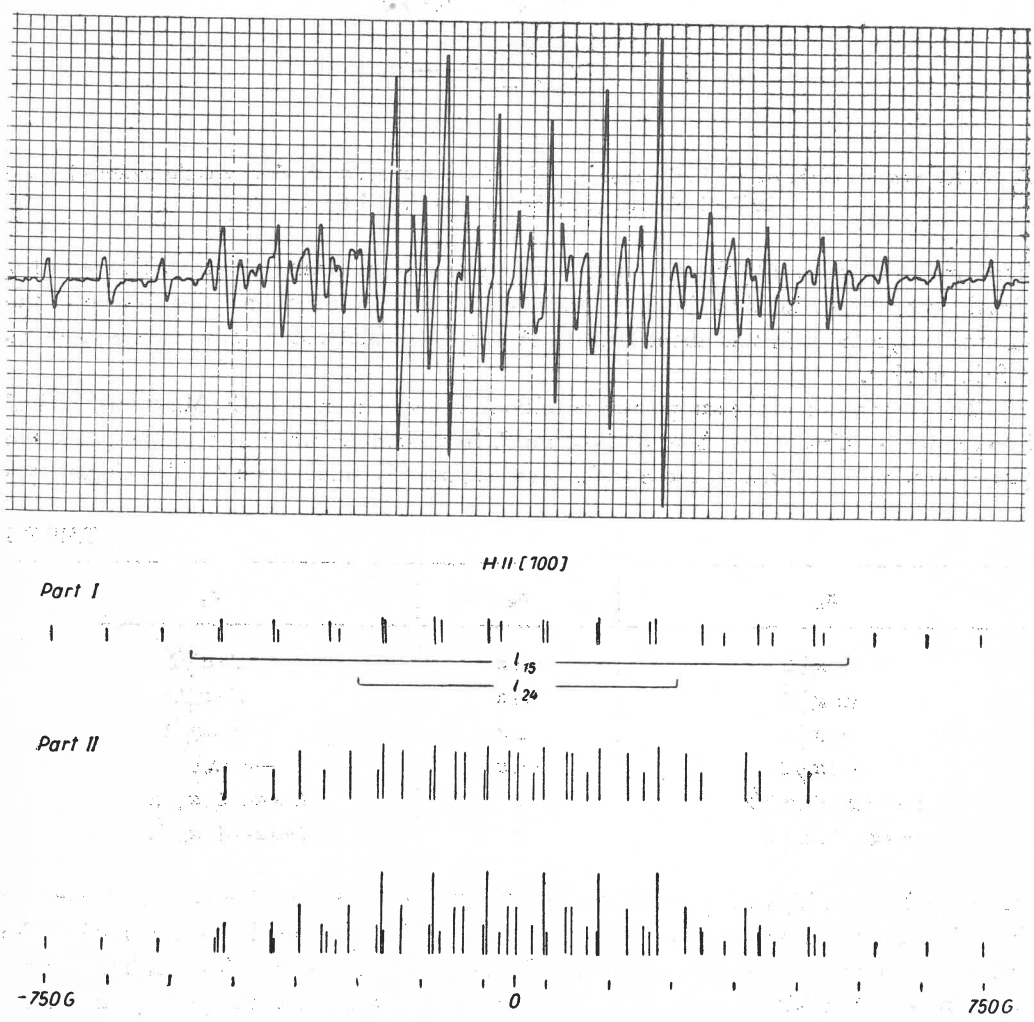

Fig. 4a

Experimental results

The experiment consists of two parts. One is the measurement of the resonance spectrum needed for the calculation of the spin Hamiltonian parameters A, a, D, E. The other is the observation of the angular dependence of the fine structure lines.

In order to evaluate the parameters the paramagnetic resonance spectrum for two orientations were observed. These were $\alpha = 0°$ and $\alpha = 45°$ (Fig. 4 *a* and *b*). $\alpha = 0°$ corres-

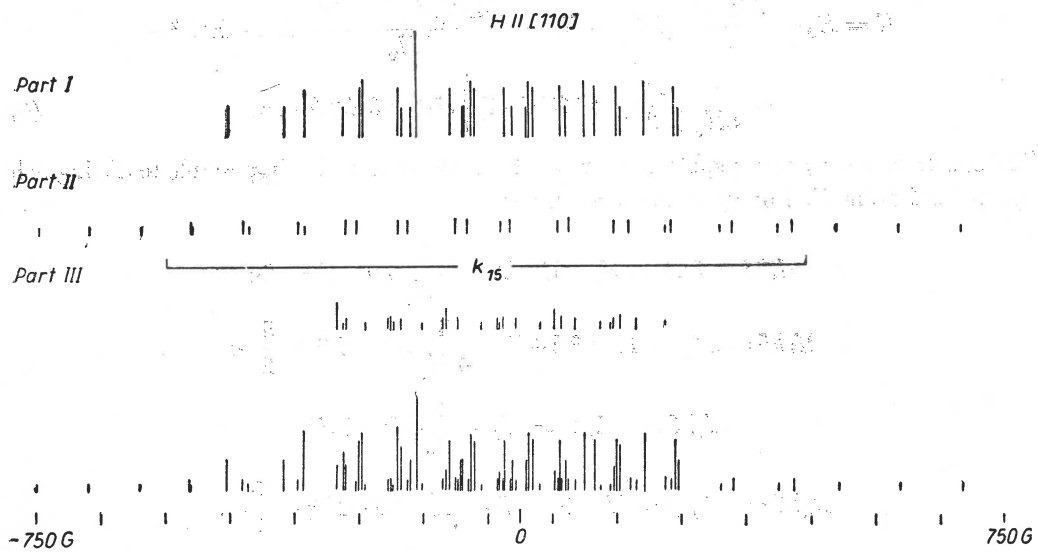

Fig. 4*b*

Fig. 4*a*, *b*. The liquid nitrogen temperature spectrum of Mn^{++} in quenched NaCl single crystal. The observed spectrum is shown in the upper part each figure, while the calculated one in the lower part. The magnetic field is along the [100] direction in Fig. 4*a* and the [110] direction in Fig. 4*b*. The calculated spectra are composed of two spectra, I and II, in Fig. 4*a* and three spectra, I, II and III, in Fig. 4*b*. From the spectra the spin Hamiltonian constants a, E, D are calculated

ponds to H parallel to the [100] cubic axis. Then the absolute values of the direction cosines (for $\alpha = 0°$) of the magnetic field with respect to the direction of the vacancy-Mn^{++} complex are as follows:

TABLE II

n_x	n_y	n_z	
0	1	0	Part I
0	1	0	
$1/\sqrt{2}$	0	$1/\sqrt{2}$	
$1/\sqrt{2}$	0	$1/\sqrt{2}$	Part II
$1/\sqrt{2}$	0	$1/\sqrt{2}$	
$1/\sqrt{2}$	0	$1/\sqrt{2}$	

In this case there are only two different orientations of the vacancy-Mn^{++} complex and the spectrum is composed of two parts (Fig. 4*a*). Taking into account only the fine structure the resonance fields can be written as
part I

$$H = H_0 + \frac{2M+1}{2}(D+3E) - \frac{1}{8H_0}\left[\frac{29}{2} - 6M(M+1)\right](D-E)^2 + ca \tag{5}$$

and part II

$$H = H_0 - \frac{2M+1}{2}(D/2+3E/2) - \frac{24M(M+1)-26}{2H_0}(D/2-E/2)^2 - \\ - \frac{1}{8H_0}\left[\frac{29}{2} - 6M(M+1)\right](D/2+3E/2)^2 + ca. \tag{6}$$

The spectrum I has greater splitting than spectrum II, what makes it possible to distinguish spectrum I from II. For spectrum I we have:

$$H(M = 3/2) = H_0 + 6E + 2D + \frac{1}{H_0}(D-E)^2 - 2a$$

$$H(M = 1/2) = H_0 + 3E + D - \frac{5}{4H_0}(D-E)^2 + \frac{5}{2}a$$

$$H(M = -1/2) = H_0 - \frac{2}{H_0}(D-E)^2$$

$$H(M = -3/2) = H_0 - 3E - D - \frac{5}{4H_0}(D-E)^2 - \frac{5}{2}a$$

$$H(M = -5/2) = H_0 - 6E - 2D + \frac{1}{H_0}(D-E)^2 + 2a. \tag{7}$$

Hence,

$$a = \frac{2l_{24} - l_{15}}{14} \tag{8}$$

and

$$3E+D=\frac{5l_{15}+4l_{24}}{28} \tag{9}$$

where

$$l_{24}=H(M=1/2)-H(M=-3/2) \text{ and } l_{15}=H(M=3/2)-H(M=-5/2)$$

for spectrum I (Fig. 4*a*).

For calculation of the parameters E and D the next spectrum with $\alpha=45°$ has to be regarded (Fig. 4*b*). Then the absolute values of direction cosines of magnetic field with respect to the direction of the vacancy-Mn^{++} complex are as follows:

TABLE III

n_x	n_y	n_z	
1/2	$1/\sqrt{2}$	1/2	
1/2	$1/\sqrt{2}$	1/2	
1/2	$1/\sqrt{2}$	1/2	Part I
1/2	$1/\sqrt{2}$	1/2	
0	0	1	Part II
1	0	0	Part III

In this case there are three different spectra corresponding to the three orientations of the Mn^{++}-vacancy complex. As before, one of the spectra, II, has a greater splitting and can be easily distinguished from other two. The expression for obtaining the parameters D and E now has the form

$$8D=4a-k_{15}, \tag{10}$$

where $k_{15}=H(M=3/2)-H(M=-5/2)$ for spectrum II.

That is to say that by measuring the distances between the corresponding fine structure lines (or rather between the centers of the hyperfine structure group) we can calculate the absolute values of parameters a, E, D.

The absolute value of the hyperfine constant A can be evaluated from any orientation of magnetic field because it is nearly isotropic. A can be directly found by measuring the separations between the suitable hyperfine lines (the diagonal of the Table IV).

The absolute signs of the constants can not be obtained from EPR measurements alone. Only the relative signs can be determined in this case. The sign of A has been obtained from second order efects. The hyperfine structure separation within a group increases by about 2—3 G ($A^2/H_0=2.4$ G from theoretical predictions, Table IV) per each separation towards increasing magnetic field. That is A has a negative sign.

The signs of D and E were determined by considering the variation of the spacings of his multiplets assuming that A is negative [11]. From the experimental data the overall

TABLE IV

Separations between hfs lines

Numbers of successive lines \ M	$-5/2$	$-3/2$	$-1/2$	$1/2$	$3/2$
2–1	$-A$	$-A-A^2/H_0$	$-A-2A^2/H_0$	$-A-3A^2/H_0$	$-A-4A^2/H_0$
3–2	$-A+A^2/H_0$	$-A$	$-A-A^2/H_0$	$-A-2A^2/H_0$	$-A-3A^2/H_0$
4–3	$-A+2A^2/H_0$	$-A+A^2/H_0$	$-A$	$-A-A^2/H_0$	$-A-2A^2/H_0$
5–4	$-A+3A^3/H_0$	$-A+2A^2/H_0$	$-A+A^2/H_0$	$-A$	$-A-A^2/H_0$
6–5	$-A+4A^2/H_0$	$-A+3A^2/H_0$	$-A+2A^2/H_0$	$-A+A^2/H_0$	$-A$

splitting in each hfs group decreases with increasing field. From the hyperfine part of Eg. (4) it follows that the line corresponding to $m = 5/2$ should lie at a field greater than that for $m = 5/2$ by

$$-5A-(5A^2/2H_0)\,(2M+1). \tag{11}$$

The modulus of this is greater for negative M because A is negative. This means that the transitions with negative M appear in low magnetic fields, while those with positive M in high fields for part I and *vice versa* for part II (Fig. 4*a*). Reference to Eq. (4) and the experimental fact that the total splitting of resonance spectrum is about 1500 G show that D and E have the same sign. According to Eqs (7) and the fact that the transitions with negative M appear in low field for the part $I(\alpha = 0)$, the signs of D and E are positive. The same conclusions about the signs of the D and E can be obtained for the other cases. The sign of a was assumed to be negative, what is consistent with the previous calculations of a, D, E from Eqs (8), (9), (10).

TABLE V

Spin Hamiltonian constants for Mn^{++} in NaCl

Temperature	g	$A(G)$	$a(G)$	$D(G)$	$E(G)$	References
77° K	...	−87.9	−2.4	124.3	46.2	this work
298° K	2.0021	$A_x = A_y = 88.4$ $A_z = 88.7$	−1.4	−144.5	43.5	Watkins
300° K	2.0012	−88.7	—	137.9	51.4	Morigaki

The spin Hamiltonian constants are given in Table V. Watkins [19] accepted a coordinate system in which the z-axis is along the cubic axis and the x-axis is in the direction of the Mn^{++}-vacancy complex. Therefore, he has different values of D and E constants. Moreover Morigaki *et al.* [7] did not take into account the quartic terms of Eq. (3) with a constant. The temperature dependence of D and E has been studied by Pfister *et al.* [12].

The second part of the experiment consisted in the observation of the angular dependence of the spectrum. The spectrum is very sensitive to the angle between the cubic axis

and the magnetic field. Even a small change of orientation induces a significant change in the spectrum. This is easily understood from Fig. 5. The figure shows the angular dependence of the position of a fine structure line with $M = -3/2$ with respect to the line with $M = -5/2$ calculated from Eq. (4) without its hfs part. The curve designated I corresponds to the z-axis at [011] or [01$\bar{1}$], curve II — at [101] or [$\bar{1}$01], curve III — at [110]

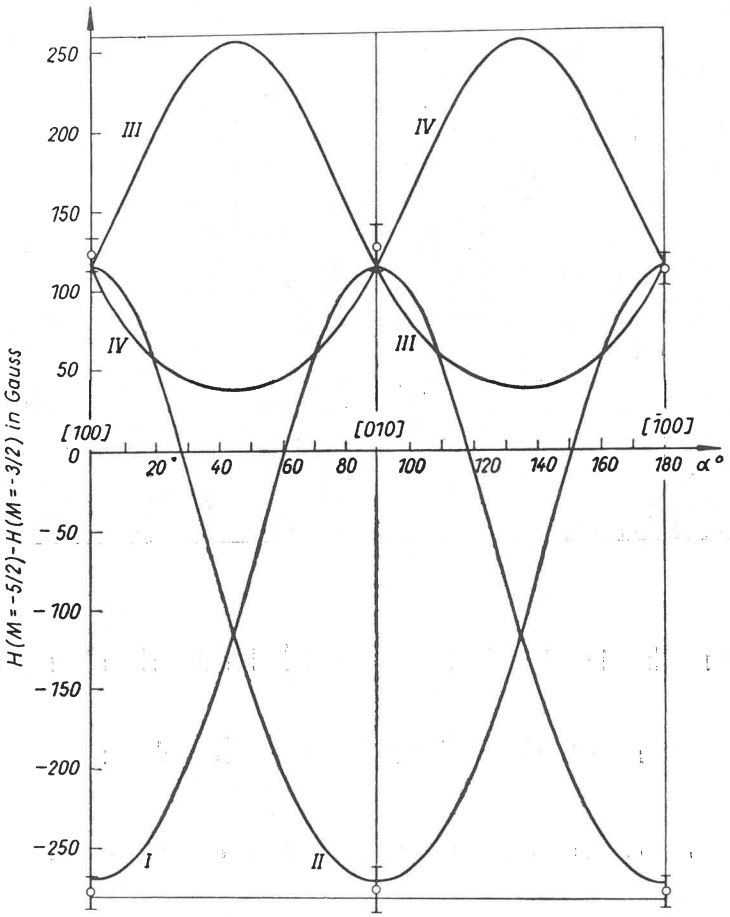

Fig. 5. The theoretical angular dependence of differences between the resonance fields of two fine structure lines: $H(M = -5/2) - H(M = 3/2)$ in NaCl:Mn^{++} crystal (solid curves) and experimental points (circles)

and IV —at the [1$\bar{1}$0] direction. The plot of Fig. 5 has the twofold symmetry (symmetry axes for $\alpha = 0°$ and $\alpha = 180°$). The observed spectrum has the fourfold symmetry. This is in full agreement with the theoretical calculation because of the identical dependence of line position on angle α for curves I and II and for curves III and IV, what gives in the latter the fourfold symmetry in the calculated spectrum.

The analogous angular dependence were calculated and observed for positions of the other fine structure lines. From Fig. 5 it is seen that a small change of α gives a big change

in position of the fine structure lines. Remembering that the splitting of each fine structure line for the six hfs components occurs, we can predict a significant sensitivity of the spectrum on orientation in the magnetic field. This fact is actually observed and presents considerable difficulties in the distinction of the four (in the general case) different orientations of z-axis for a definite angle α, (for example, see Fig. 6). Thus, only some of the experimental points are ploted in Fig. 5.

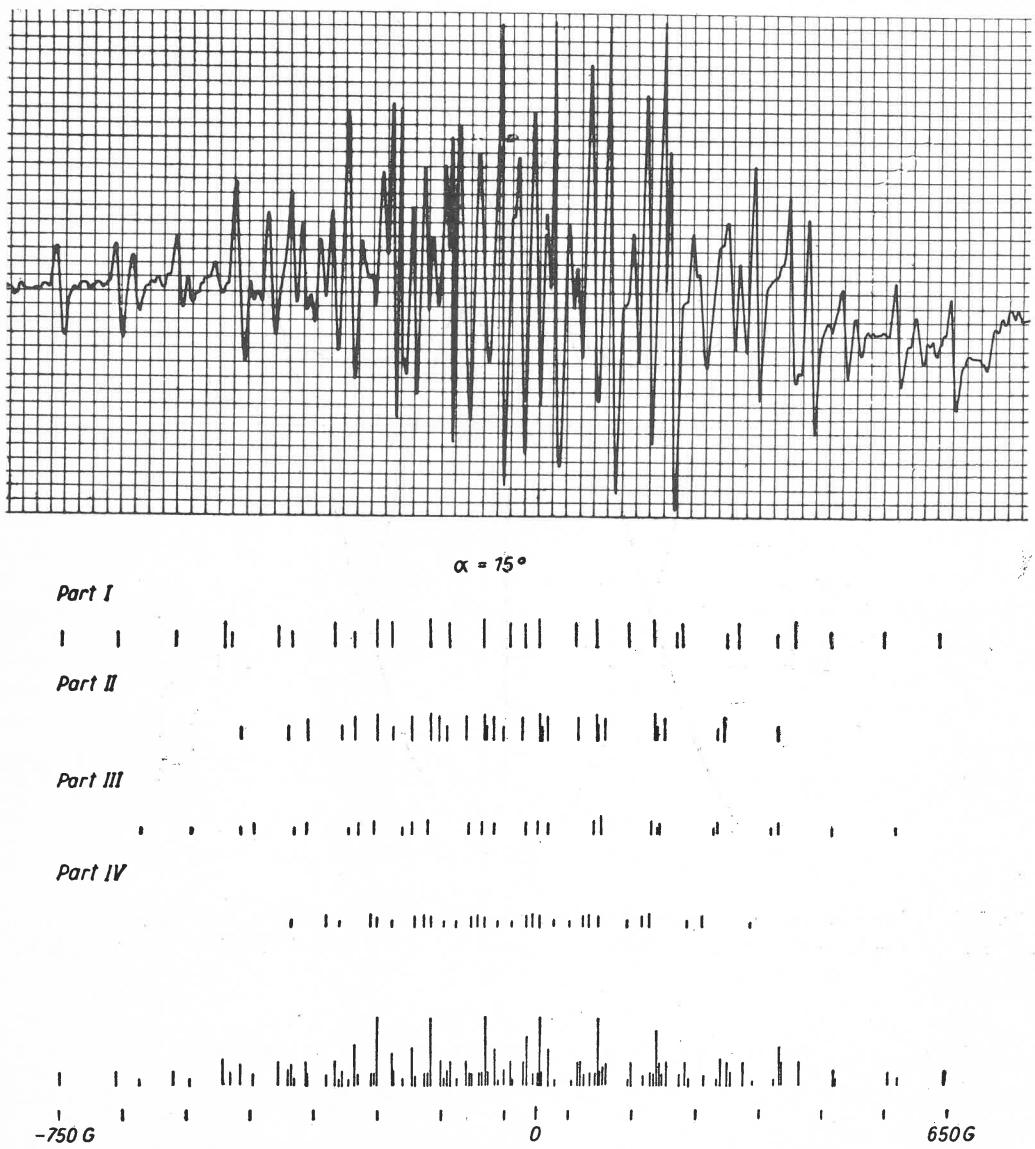

Fig. 6. The liquid nitrogen temperature spectrum of Mn^{++} in quenched NaCl single crystal. The observed spectrum is shown in the upper part of figure, while the calculated one in the lower part. The magnetic field makes an angle $\alpha = 15°$ with the (1) cubic axis. The calculated spectra are composed of four parts

Other features of the spectrum

Other spectra. Thermal treatment

Apart from the dominant spectrum described previously there are other spectra which can be observed in NaCl : Mn^{++} crystals. The spectrum designated I (according to [19]) consists of a single broad line corresponding to precipitated Mn^{++} ions. The spectrum I is observed in crystals without heating. The spectrum is independent of orientation of the crystal in the magnetic field.

With the single crystal quenched from high temperature to room temperature many strongly orientation-dependent lines are observed at room and liquid nitrogen temperatures. The spectrum consists of several parts and is associated with isolated Mn^{++} ions in different lattice environments. Thus, the spectrum II corresponds to isolated Mn^{++} ions which are not near any defect and, therefore, have local cubic symmetry. The orthorhombic spectrum III_1 (presented in this paper) corresponds to isolated Mn^{++} ion associated with the nearest neighbouring Na^+-vacancy, while the tetragonal III_2 spectrum is associated with a second nearest Na^+-vacancy. The orthorhombic spectrum IV is caused by an associated Mn^{++}-X^{--} pair (where X^{--} is an unknown negative impurity at the nearest Cl^- site). The orthorhombic spectrum V observed by Shrivastava and Venkateswarlu [13] and [14] is connected with an associated Mn^{++}-O^{--} pair and a second neighbouring cation vacancy. Finally the tetragonal spectrum VI (also observed by Shrivastava and Venkateswarlu) is due to an Mn^{++} ion associated with a point defect in which the nearest Cl^- ion is replaced by an OH^- ion and probably with a second neighbouring cation vacancy. The last spectrum disappear after quenching.

Several hours after heating the complicated spectrum disappears and the spectrum I increases, what means that the initially isolated (after quenching) Mn^{++} ions are now in close proximity to each other, aggregate at or near internal boundaries or dislocations. The process of precipitating and dissolving Mn^{++} ions is reversible, of course.

The temperature dependence (in the 300°K to 720°K region) of the Mn^{++} spectrum in quenched NaCl was observed by Watkins [9]. As the temperature is raised from the room temperature most of the lines grow and at 720°K only the six central lines, corresponding to the spectrum II remain.

In recent years experiments with NaCl : Mn^{++} single crystals also revealed spectra of new centres after irradiation [15], [16] and [17] and the influence of electric fields on the splitting of the $^6S_{5/2}$ Mn^{++} ground state [18] and [19].

In this paper only the spectra I and III_1 were observed.

Plastic deformation

Plastic deformation of NaCl : Mn^{++} crystals has been the subject of a number of papers [20–23]. Alzetta *et al.* observed the spectrum I before and after plastic deformation at room temperature. After deformation the six lines of the hyperfine structure of Mn^{++} are recognized on the broad line.

Santucci and Alzetta also observed the change of the resonance spectrum III after plastic deformation. The same experiments were made by the author. The compression at room temperature was applied in the direction normal to the lattice planes. Deformation was

measured by means of a micrometric screw and amounted to 5–15%, but no changes in the spectra I and III_1 were observed. The spectrum III_1 is very complicated and strongly dependent on orientation, so this is not good material for studying deformation.

Therefore plastic deformation will be studied later for NaCl crystals doped with other impurities of the iron group which give simpler spectra.

Conclusion

The measurements reported in this paper have yielded information on vacancy defects in $NaCl:Mn^{++}$ single crystals. They point to the fact that at room temperature before quenching most of the Mn^{++} ions are not in solution but in some type of aggregated state. After quenching, the Mn^{++} ions are dissolved into the lattice and give a spectrum which corresponds to a positive ion vacancy in the nearest Mn^{++} position.

It was observed that the crystals containing a smaller amount of impurity are more "stable" than those with high concentrations of impurity at room temperature. The NaCl crystal containing a 1% mole fraction of Mn^{++} doped into the melt has some precipitated ions already one hour after quenching, while those of 0.1% mole fraction — after 3–4 hours. This fact is in a good agreement with the known mechanism of cation diffusion in NaCl crystals [24]. At temperature below 550°C the cation vacancies and the impurity-vacancy complex participate equally in the cation diffusion process. A smaller concentration of Mn^{++} ions gives a smaller number of vacancies and impurity-vacancy complexes, so the diffusion of the manganese ions is obviously slower. The process of diffusion in quenched samples become "frozen" at liquid nitrogen temperature, what was also observed.

I am greatly indebted to Professor K. Leibler for helpful discussions and comments. Thanks are also due to Mr I. Olichwierowicz, who prepared the crystals, and Miss W. Gniado for numerical calculations on the Odra 1013 computer.

REFERENCES

[1] K. K. Shwarc, W. B. Laizan, A. F. Lushina, *Radiatsonnaya Fizika*, 1964.
[2] V. B. Laizan, A. I. Vitol, *Radiatsonnaya Fizyka i Ionnye Kristaly*, Izd. Ak. Nauk. Lotw. SSR, Ryga 1964.
[3] G. Alzetta, P. R. Crippa, S. Santucci, *Nuovo Cimento*, **42 B**, 100 (1966).
[4] M. I. Kornfeld, I. N. Tolparov, *Fiz. Tverdogo Tela*, **9**, 2047 (1967).
[5] E. E. Schneider, J. E. Caffyn, *Defects in Crystalline Solids*, Report of Bristol Conference, London Phys. Soc., p. 74, 1955.
[6] P. A. Forrester, E. E. Schneider, *Proc. Phys. Soc.*, **B69**, 833 (1856).
[7] K. Morigaki, M. Fujimoto, J. Itoh, *J. Phys. Soc. Japan*, **13**, 1174 (1958).
[8] G. D. Watkins, R. M. Walker, *Bull. Amer Phys. Soc.*, II, **1**, 324 (1956).
[9] G. D. Watkins, *Phys. Rev.*, **113**, 79 (1959).
[10] G. D. Watkins, *Phys. Rev.*, **113**, 91 (1959).
[11] B. Bleaney, D. J. E. Ingram, *Proc. Roy. Soc.*, **A205**, 336 (1951).
[12] G. Pfister, W. Dreybrodt, W. Assmus, *Phys. Status Solidi*, **36**, 351 (1969).
[13] K. N. Shrivastava, *Phys. Letters*, **26A**, 251 (1968).
[14] K. N. Shrivastava, P. Venkateswarlu, *Proc. Indian Acad. Sci.*, **63A**, 284 (1966).
[15] P. Bettica, S. Santucci, A. Stefanini, *Nuovo Cimento*, **48**, 316 (1967).

[16] M. Ykeya, N. Itoh, *Solid State Commun.*, **7**, 355 (1969).
[17] M. Ykeya, N. Itoh, *J. Phys. Soc. Japan*, **26**, 291 (1969).
[18] W. Dreybrodt, G. Pfister, *Phys. Status Solidi*, **34**, 69 (1969).
[19] W. Dreybrodt, D. Silber, *Phys. Status Solidi*, **34**, 559 (1969).
[20] G. Alzetta, P. R. Crippa, S. Santucci, *Phys. Status Solidi*, **12**, K 81 (1965).
[21] H. Kawamura, Y. Okubo, *J. Appl. Phys.*, **33** supl., 367 (1962).
[22] S. Santucci, G. Alzetta, *Consiglio Nazionale delle Ricerche*, Convegno-Pavia 1962, Roma 1964.
[23] M. Ueta, W. Kanzig, *Phys. Rev.*, **97**, 1591 (1955).
[24] L. A. Grifalco, *Atomic Migration in Crystals*, Blaisd. Publ. Co., 1964.